ISSN 1948-5204 (online)

World Journal of *Gastrointestinal Oncology*

World J Gastrointest Oncol 2019 December 15; 11(12): 1092-1239

Published by Baishideng Publishing Group Inc

WJGO

World Journal of Gastrointestinal Oncology

Contents

Monthly Volume 11 Number 12 December 15, 2019

OPINION REVIEW

1092 Observation or resection of pancreatic intraductal papillary mucinous neoplasm: An ongoing tug of war
Aunan JR, Jamieson NB, Søreide K

MINIREVIEW

1101 Current status of the genetic susceptibility in attenuated adenomatous polyposis
Lorca V, Garre P

ORIGINAL ARTICLE

Basic Study

1115 Improved method for inducing chronic atrophic gastritis in mice
Wei X, Feng XP, Wang LY, Huang YQ, Liang LL, Mo XQ, Wei HY

Case Control Study

1126 Relationship between cachexia and perineural invasion in pancreatic adenocarcinoma
Petrusel L, Rusu I, Leucuta DC, Seicean R, Suharoschi R, Zamfir P, Seicean A

1141 Protein expression trends of DNMT1 in gastrointestinal diseases: From benign to precancerous lesions to cancer
Ma TM, Sun LP, Dong NN, Sun MJ, Yuan Y

Retrospective Study

1151 Asian Americans have better outcomes of non-metastatic gastric cancer compared to other United States racial groups: A secondary analysis from a randomized study
Abdel-Rahman O

1161 Gastric partitioning for the treatment of malignant gastric outlet obstruction
Ramos MFKP, Barchi LC, de Oliveira RJ, Pereira MA, Mucerino DR, Ribeiro Jr U, Zilberstein B, Cecconello I

1172 Difference in failure patterns of pT3-4N0-3M0 esophageal cancer treated by surgery *vs* surgery plus radiotherapy
Zeng Y, Yu W, Liu Q, Yu WW, Zhu ZF, Zhao WX, Liu J, Wang JM, Fu XL, Liu Y, Cai XW

Observational Study

1182 Impact of regular enteral feeding *via* jejunostomy during neo-adjuvant chemotherapy on body composition in patients with oesophageal cancer
Mohamed IM, Whiting J, Tan BH

1193 Multi-parameter ultrasound based on the logistic regression model in the differential diagnosis of hepatocellular adenoma and focal nodular hyperplasia

Wu M, Zhou RH, Xu F, Li XP, Zhao P, Yuan R, Lan YP, Zhou WX

1206 Analysis of factors potentially predicting prognosis of colorectal cancer

Jin LJ, Chen WB, Zhang XY, Bai J, Zhao HC, Wang ZY

SYSTEMATIC REVIEWS

1218 Deep learning with convolutional neural networks for identification of liver masses and hepatocellular carcinoma: A systematic review

Azer SA

CASE REPORT

1231 Inflammatory pseudotumor-like follicular dendritic cell sarcoma: A brief report of two cases

Zhang BX, Chen ZH, Liu Y, Zeng YJ, Li YC

Contents

World Journal of Gastrointestinal Oncology

Volume 11 Number 12 December 15, 2019

ABOUT COVER

Editorial Board Member of *World Journal of Gastrointestinal Oncology*, Paolo Aurello, MD, PhD, Professor, Surgeon, Department of General Surgery, Sapienza University of Rome, Rome 00162, Italy

AIMS AND SCOPE

The primary aim of *World Journal of Gastrointestinal Oncology* (*WJGO*, *World J Gastrointest Oncol*) is to provide scholars and readers from various fields of gastrointestinal oncology with a platform to publish high-quality basic and clinical research articles and communicate their research findings online.

WJGO mainly publishes articles reporting research results and findings obtained in the field of gastrointestinal oncology and covering a wide range of topics including islet cell adenoma, liver cell adenoma, adenomatous polyposis coli, appendiceal neoplasms, bile duct neoplasms, biliary tract neoplasms, hepatocellular carcinoma, islet cell carcinoma, pancreatic ductal carcinoma, cecal neoplasms, colonic neoplasms, colorectal neoplasms, hereditary nonpolyposis colorectal neoplasms, common bile duct neoplasms, duodenal neoplasms, esophageal neoplasms, gallbladder neoplasms, *etc*.

INDEXING/ABSTRACTING

The *WJGO* is now indexed in Science Citation Index Expanded (also known as SciSearch®), PubMed, and PubMed Central. The 2019 edition of Journal Citation Reports® cites the 2018 impact factor for *WJGO* as 2.758 (5-year impact factor: 3.220), ranking *WJGO* as 52 among 84 journals in gastroenterology and hepatology (quartile in category Q3), and 131 among 229 journals in oncology (quartile in category Q3).

RESPONSIBLE EDITORS FOR THIS ISSUE

Responsible Electronic Editor: *Lu-Lu Qi*

Proofing Production Department Director: *Yun-Xiaojian Wu*

NAME OF JOURNAL
World Journal of Gastrointestinal Oncology

ISSN
ISSN 1948-5204 (online)

LAUNCH DATE
February 15, 2009

FREQUENCY
Monthly

EDITORS-IN-CHIEF
Monjur Ahmed, Rosa M Jimenez Rodriguez, Pashtoon Kasi

EDITORIAL BOARD MEMBERS
https://www.wjgnet.com/1948-5204/editorialboard.htm

EDITORIAL OFFICE
Jin-Lei Wang, Director

PUBLICATION DATE
December 15, 2019

INSTRUCTIONS TO AUTHORS
https://www.wjgnet.com/bpg/gerinfo/204

GUIDELINES FOR ETHICS DOCUMENTS
https://www.wjgnet.com/bpg/GerInfo/287

GUIDELINES FOR NON-NATIVE SPEAKERS OF ENGLISH
https://www.wjgnet.com/bpg/gerinfo/240

PUBLICATION MISCONDUCT
https://www.wjgnet.com/bpg/gerinfo/208

ARTICLE PROCESSING CHARGE
https://www.wjgnet.com/bpg/gerinfo/242

STEPS FOR SUBMITTING MANUSCRIPTS
https://www.wjgnet.com/bpg/GerInfo/239

ONLINE SUBMISSION
https://www.f6publishing.com

World Journal of Gastrointestinal Oncology

Submit a Manuscript: https://www.f6publishing.com

World J Gastrointest Oncol 2019 December 15; 11(12): 1193-1205

DOI: 10.4251/wjgo.v11.i12.1193

ISSN 1948-5204 (online)

ORIGINAL ARTICLE

Observational Study

Multi-parameter ultrasound based on the logistic regression model in the differential diagnosis of hepatocellular adenoma and focal nodular hyperplasia

Meng Wu, Ru-Hai Zhou, Feng Xu, Xian-Peng Li, Ping Zhao, Rui Yuan, Yu-Peng Lan, Wei-Xia Zhou

ORCID number: Meng Wu (0000-0001-8840-8753); Ru-Hai Zhou (0000-0002-3254-1742); Feng Xu (0000-0001-3379-8480); Xian-Peng Li (0000-0001-1580-5325); Ping Zhao (0000-0002-5689-4358); Rui Yuan (0000-0001-7543-8954); Yu-Peng Lan (0000-0001-4704-3250); Wei-Xia Zhou (0000-0001-8653-0451).

Author contributions: Wu M, Zhou RH, Xu F, Li XP, Zhao P and Yuan R designed research; Wu M, Xu F, Zhao P and Lan YP performed research; Lan YP and Zhou WX contributed new analytic tools; Zhou RH, Li XP, Yuan R and Zhou WX analyzed data; and Wu M, Zhou RH, Xu F, Lan YP and Zhou WX wrote the paper.

Supported by Zhejiang Natural Science Foundation, NO. LY16H160004; Ningbo Yinzhou District Agricultural and Social Development Science and Technology Project, NO. Yinke 2018-74.

Institutional review board statement: The study was approved by the ethics committee of Yinzhou Hospital affiliated to Ningbo University School of Medicine.

Informed consent statement: Patients were not required to give informed consent to the study because the analysis used anonymous clinical data that were obtained after each patient agreed to treatment by written consent.

Meng Wu, Ru-Hai Zhou, Feng Xu, Xian-Peng Li, Ping Zhao, Rui Yuan, Yu-Peng Lan, Wei-Xia Zhou, Department of Ultrasound, Yinzhou Hospital Affiliated to Ningbo University School of Medicine, Ningbo 315000, Zhejiang Province, China

Feng Xu, Xian-Peng Li, Department of Gastroenterology, Yinzhou Hospital Affiliated to Ningbo University School of Medicine, Ningbo 315000, Zhejiang Province, China

Corresponding author: Meng Wu, MD, Doctor, Department of Ultrasound, Yinzhou Hospital affiliated to Ningbo University School of Medicine, No. 251 Baizhang East Road, Ningbo 315040, Zhejiang Province, China. wumengcool@sina.com
Telephone: +86-574-87017240

Abstract

BACKGROUND

Focal nodular hyperplasia (FNH) has very low potential risk, and a tendency to spontaneously resolve. Hepatocellular adenoma (HCA) has a certain malignant tendency, and its prognosis is significantly different from FNH. Accurate identification of HCA and FNH is critical for clinical treatment.

AIM

To analyze the value of multi-parameter ultrasound index based on logistic regression for the differential diagnosis of HCA and FNH.

METHODS

Thirty-one patients with HCA were included in the HCA group. Fifty patients with FNH were included in the FNH group. The clinical data were collected and recorded in the two groups. Conventional ultrasound, shear wave elastography, and contrast-enhanced ultrasound were performed, and the lesion location, lesion echo, Young's modulus (YM) value, YM ratio, and changes of time intense curve (TIC) were recorded. Multivariate logistic regression analysis was used to screen the indicators that can be used for the differential diagnosis of HCA and FNH. A ROC curve was established for the potential indicators to analyze the accuracy of the differential diagnosis of HCA and FNH. The value of the combined indicators for distinguishing HCA and FNH were explored.

RESULTS

Multivariate logistic regression analysis showed that lesion echo (P = 0.000), YM

Conflict-of-interest statement: None of the authors have any conflict of interest to disclose.

Manuscript source: Unsolicited manuscript

Received: June 15, 2019
Peer-review started: June 18, 2019
First decision: July 31, 2019
Revised: August 13, 2019
Accepted: September 10, 2019
Article in press: September 10, 2019
Published online: December 15, 2019

P-Reviewer: Ryan EM, Shaun C, Satya R
S-Editor: Zhang L
L-Editor: Filipodia
E-Editor: Qi LL

value (P = 0.000) and TIC decreasing slope (P = 0.000) were the potential indicators identifying HCA and FNH. In the ROC curve analysis, the accuracy of the YM value distinguishing HCA and FNH was the highest (AUC = 0.891), which was significantly higher than the AUC of the lesion echo and the TIC decreasing slope (P < 0.05). The accuracy of the combined diagnosis was the highest (AUC = 0.938), which was significantly higher than the AUC of the indicators diagnosing HCA individually (P < 0.05). This sensitivity was 91.23%, and the specificity was 83.33%.

CONCLUSION
The combination of lesion echo, YM value and TIC decreasing slope can accurately differentiate between HCA and FNH.

Key words: Hepatocellular adenoma; Focal nodular hyperplasia; Ultrasound; Logistic regression

Core tip: The prognosis of hepatocellular adenoma (HCA) is significantly different from focal nodular hyperplasia (FNH). Accurate identification of HCA and FNH is of great significance. This study explored the accuracy of the combined detection of HCA and FNH by conventional ultrasound, shear wave elastography, and contrast-enhanced ultrasound. The combination of lesion echo, Young's modulus value and time intense curve decreasing slop in multi-parameter ultrasound index based on logistic regression has high clinical guiding value for the differential diagnosis of HCA and FNH.

Citation: Wu M, Zhou RH, Xu F, Li XP, Zhao P, Yuan R, Lan YP, Zhou WX. Multi-parameter ultrasound based on the logistic regression model in the differential diagnosis of hepatocellular adenoma and focal nodular hyperplasia. *World J Gastrointest Oncol* 2019; 11(12): 1193-1205
URL: https://www.wjgnet.com/1948-5204/full/v11/i12/1193.htm
DOI: https://dx.doi.org/10.4251/wjgo.v11.i12.1193

INTRODUCTION

Focal nodular hyperplasia (FNH) is a proliferative lesion caused by vascular malformation, which is very common in the clinic. The potential risk is extremely low, most of FNH will not be malignant, and it has a tendency to spontaneously resolve[1-3]. Hepatocellular adenoma (HCA) is a rare liver tumor, which is prone to secondary hemorrhage and has a tendency towards malignant transformation. Although it can be treated conservatively after diagnosis, it must be closely monitored. Surgical resection is required once it is considered to be malignant, and its prognosis is also significantly different from FNH[4-6]. Therefore, accurate identification of HCA and FNH is essential for clinical treatment. However, patients with HCA or FNH have no obvious clinical symptoms, and tumor markers are not significantly expressed in FNH or HCA[7-9]. Ultrasound is a routine imaging diagnostic tool for diagnosing liver diseases. Although traditional two-dimensional ultrasound and Doppler ultrasound are difficult to distinguish, recent research has revealed that contrast-enhanced ultrasound (CEUS) has a certain value in this identification[10,11]. CEUS can clearly identify FNH and HCA through stellate scars in the central part of small FNH[12]. However, due to the low incidence of HCA, the CEUS performance of FNH is not typical. Hence, the value of CEUS in identifying HCA and FNH is limited currently[13,14]. In recent years, real-time shear wave elastography (SWE) technology can non-invasively and accurately obtain the absolute elasticity value of diseased tissues, and has been applied to the differential diagnosis of benign and malignant liver-occupying lesions[15-17]. To date, however, SWE has less application in identifying HCA and FNH. In the study of Gerber *et al*[18], the hardness of FNH was higher than HCA, but the sample size was insufficient and needed further verification[18]. Therefore, this study recruited HCA and FNH patients as research subjects. It systematically analyzed the different performances of conventional ultrasound, SWE and CEUS between HCA and FNH, and explored the value of ultrasound multi-

parameter indicators in the differential diagnosis of HCA and FNH. Furthermore, a logistic regression model was used to establish a combined diagnosis of ultrasound multi-parameter indicators. The value of multi-parameter combined identification of HCA and FNH was explored to provide useful information for the follow-up treatment of HCA.

MATERIALS AND METHODS

Research objective

Patients diagnosed with HCA or FNH in Yinzhou Hospital affiliated with Ningbo University School of Medicine from January 2017 to September 2019 were recruited. Inclusion criteria were as follows: (1) Diagnosed as HCA or FNH by surgical pathology or biopsy; and (2) Underwent color Doppler ultrasound, SWE, and CEUS examination, as well as obtained complete imaging data before surgery. Patients with malignant tumors or severe liver, kidney, heart, and brain dysfunction were excluded. A total of 31 patients with HCA who met the criteria were divided into the HCA group, including eight males and 23 females. The age range was 20-42 years old, with an average of 27.29 ± 9.87 years. A total of 50 FNH patients were divided into the FNH group, including 24 males and 26 females. The age range was 18-years-old to 48-years-old, with an average of 28.09 ± 10.57 years. The age, gender, history of viral infection, and history of cirrhosis was recorded in the two groups. All patients gave informed consent for the study, and the study was approved by the Ethics Committee of Yinzhou Hospital affiliated with Ningbo University School of Medicine.

Research methods

Liver function and serological examination: Liver function analysis and serological examination were performed on both groups. The patients were kept on a light diet, and fasted for 8 h before examination. Blood was taken from the elbow vein in the morning. Liver function and serological parameters of the two groups were determined using a Bayerl 650 automatic biochemical analyzer. Liver function indicators included alanine aminotransferase (ALT), aspartate aminotransferase (AST), and glutamyl transpeptidase (GGT). Serological indicators included albumin, total bilirubin (Tbil), prothrombin time (PT), and serum ferritin (SF).

Tumor markers: The alpha-fetoprotein (AFP) index of the two groups was examined and recorded by chemiluminescence immunoassay. The kit was purchased from Siemens Medical Diagnostics Products (Shanghai) Co., Ltd. and operated in strict accordance with its instructions. The AFP reference values were as follows: < 20 μg/L indicated normal; 25-100 μg/L indicated a low-level increase; 100-500 μg/L indicated a medium-level increase; > 500 μg/L indicated a high-level increase[19].

Ultrasound examination

Conventional ultrasound: An Esaote MyLab 90 (Esaote Group, Italy) color Doppler ultrasound system with 1-8 MHz frequency was used in this study. The patient was placed in a supine position with arms raised to expose the abdomen. An intercostal space scan was applied with a conventional two-dimensional ultrasound mode, and the image was adjusted after detecting the lesion to avoid rib and lung interference. The best display area of the lesion was located. Lesion location, internal echo, echo uniformity, lesion property, morphology, border, posterior echo, surrounding capsule and microcalcification were recorded. Then, the color Doppler mode was switched to observe the blood supply in the center of and surrounding the lesion.

Ultrasound elastography: SWE studies were performed using the Aixplorer™ ultrasound system (SuperSonic Imagine S.A., Aix-en-Provence, France) with a 6-8 MHz probe. The location of the lesion was determined after routine ultrasound examination. We first set the size of the sampling frame to completely cover the lesion. Meanwhile, we avoided the heart and abdominal large blood vessels. After the sampling frame was set, the patient was asked to hold for 3 s to save the SWE image. In the SWE image, the hard tissue is represented by red, and the soft tissue is represented by blue[20]. The Young's modulus (YM) value (kPa) and YM ratio were measured at the end of the examination.

CEUS examination: An Esaote MyLab 90 (Esaote Group, Italy) color Doppler ultrasound system with 1-4 MHz frequency was used for CEUS. The mechanical index was set to 0.19 and the dynamic range was 80 dB. The contrast agent was used from SonoVue (Braeeo CO., LTD). At the beginning, 25 mg of contrast medium was dissolved in 5 ml of normal saline. A 2.4 mL suspension was then injected *via* the

superficial vein of the elbow. Finally, 5 ml of normal saline was used for washout. The intensive manifestations of lesions in the arterial phase, portal venous phase, and delayed phase were continuously observed in real time. The software can automatically plot the TIC curve and record the following parameters: Background intensity (BI), peak intensity (PI), enhancement time (ET), peak intensity Change (PI-BI), TIC increasing slope, and TIC decreasing slope.

Statistical methods

Analysis was performed using Statistical Product and Service Solutions (SPSS 19.0) software. The measurement data were expressed as x ± s, and comparisons were performed using an independent sample *t* test. The count data were expressed in case or percentage, and the chi-square test was used for comparison. Multivariate logistic regression analysis was used to screen the potential identification indexes of HCA and FNH. An ROC curve was established to analyze the accuracy of the identification of HCA and FNH. The value of the combined indicators based on a logistic regression model for distinguishing HCA and FNH were explored. The difference was considered statistically significant at $P < 0.05$.

RESULTS

In this study, 31 patients in the HCA group included 31 lesions, and 50 patients in the FNH group included 50 lesions. All patients retained complete clinical, pathological, and ultrasound imaging data.

Comparison of clinical data between the HCA and FNH groups

In the HCA group, six patients had a history of viral infection, and four patents had a history of cirrhosis. The GGT was slightly elevated. ALT, AST, Albumin, Tbil, PT, AFP and SF were normal. Compared with the FNH group, the proportion of females was higher than that of the FNH group ($P < 0.05$). The other clinical data were similar with those in the FNH group, and the differences were not statistically significant ($P > 0.05$) (Table 1).

Ultrasound and pathological features of HCA

The ultrasound images of HCA showed solid lesions with round or elliptical shapes, with clear borders and high internal echoes in most cases (Figure 1A). Blood flow signals were common in most HCA lesions (Figure 1B). SWE showed that the hardness of HCA was slightly higher than that of normal surrounding liver tissue (Figure 1C). CEUS showed a rapid and significant increase in the arterial phase, a fast washout in the portal venous phase, and an equal or low enhancement in the delayed phase (Figure 1D). In terms of pathology, the gross specimens found abundant blood vessels on the surface of the tumors. The specimens were dark purple, uniform, and a few specimens were accompanied by necrosis or bleeding in the center. Microscopically, the tumor cells were similar to the surrounding normal liver cells, but there was no portal area, portal vein and small bile duct branches in the HCA. Kupffer cells, nuclear fission phase, and complete bile duct structure were lacking in the HCA (Figure 1E).

Comparison of ultrasound characteristics between the HCA and FNH groups

By comparing the ultrasound features between the HCA and FNH groups, it can be found that the HCA lesions were mostly hyperechoic, while the FNH lesions were mostly hypoechoic. In the SWE feature, the hardness of the HCA lesion was less than that of the FNH lesion. In CEUS performance, the enhancement of HCA was mostly peripheral-centered filling, with low enhancement in the delayed phase, and hemorrhagic necrosis in some HCA lesions. The enhancement of FNH was mostly radioactively filled from the center to the periphery, with slightly high or equal enhancement in the delayed phase. Some stellate scars were found in some FNH lesions. Quantitative analysis of the ultrasound characteristics of the two groups is shown in Table 2. The high echo ratio, solid lesion ratio, and TIC decreasing slope in the HCA group were significantly higher than those in the FNH group. The YM value, YM ratio, and area under the curve (AUC) were significantly lower than those in the FNH group. The differences were statistically significant ($P < 0.05$). The differences in lesion location, lesion boundary, lesion capsule, microcalcification, posterior echo, blood flow, PI-BI, ET, and TIC increasing slope were similar, and there is no statistical significance ($P > 0.05$).

Multivariate logistic regression analysis of HCA

Multivariate logistic regression analysis was performed to explore the potential

Table 1 Comparison of clinical data between hepatocellular adenoma group and focal nodular hyperplasia group

	HCA group, n = 31	FNH group, n = 50	t/χ^2 value	P value
Age	27.29 ± 9.87	28.09 ± 10.57	0.339	0.735
Gender, male/female	8/23	24/26	3.994	0.047
History of viral infection	6%	9%	0.023	0.879
History of cirrhosis	4%	6%	0.014	0.904
ALT, U/L	24.83 ± 12.94	28.76 ± 15.38	1.185	0.239
AST, U/L	29.83 ± 12.85	26.92 ± 13.64	0.954	0.343
GGT, U/L	38.32 ± 14.08	30.84 ± 10.36	1.529	0.183
Albumin, g/L	48.23 ± 3.82	47.93 ± 3.58	0.482	0.528
Tbil, μmol/L	9.38 ± 4.83	10.63 ± 5.63	0.392	0.682
PT, s	12.86 ± 0.86	12.67 ± 0.74	1.055	0.295
AFP, μg/L	14.05 ± 5.97	12.39 ± 4.29	1.454	0.150
SF, μg/L	89.35 ± 35.24	96.32 ± 43.2	0.755	0.452

HCA: Hepatocellular adenoma; FNH: Focal nodular hyperplasia; ALT: Alanine aminotransferase; AST: Aspartate aminotransferase; GGT: Glutamyl transpeptidase; Tbil: Total bilirubin; PT: Prothrombin time; AFP: Alpha-fetoprotein; SF: Serum ferritin.

indicators identifying HCA. The results showed that gender, lesion property and YM ratio had no significant effect on the identification of HCA. The differences were not statistically significant ($P > 0.05$). The lesion echo ($P = 0.000$), YM value ($P = 0.000$) and TIC decreasing slope ($P = 0.000$) were potential indicators for identifying HCA (Table 3).

ROC curve analysis of ultrasound indicators to identify HCA and FNH

The AUC of each ultrasound indicator distinguishing HCA and FNH was different. The prediction accuracy of the YM value was the highest (AUC = 0.891). The sensitivity was 92.16%, but the specificity was low (73.28%). The AUC of TIC decreasing slope and lesion echo were lower than that of YM value, and the differences were statistically significant ($P < 0.05$). The accuracy of the combination of three ultrasound indicators identifying HCA and FNH was the highest (AUC = 0.938), which was significantly higher than the AUCs of the three ultrasound indicators individually identifying HCA and FNH. The differences were statistically significant ($P < 0.05$). The cut-off point was 0.540. Its sensitivity and specificity were 91.23% and 83.33%, respectively (Table 4 and Figure 2).

DISCUSSION

HCA is a clinically rare benign liver tumor, which often needs to be differentiated from FNH, a non-angiogenic liver benign lesion[21]. Due to the fact that the clinical symptoms of HCA and FNH are not obvious, and the level of related tumor markers are not expressed, it is difficult to differentiate them by physical examination. However, their treatments and prognoses are highly distinct[22,23]. FNH is a proliferative lesion caused by vascular malformation, whereas HCA is a dangerous tumor with a tendency to hemorrhage and undergo malignant transformation. Although a needle biopsy can be used for differential diagnosis, it is an invasive procedure and cannot be used as a routine examination. Ultrasound is important for liver examination because of its simple, non-invasive and high diagnostic accuracy. However, gray-scale ultrasound is limited in identifying HCA and FNH[24]. Although CEUS can recognize the stellate scars of FNH and the ischemic necrosis of HCA, the accuracy of CEUS in identifying HCA and FNH is not high due to the low detection rate of stellate scars of FNH[25]. As a new technique that has been widely used in the differential diagnosis of benign and malignant livers[26], SWE can be used for the differential diagnosis of FNH and HCA by detecting their YM. This study explored the accuracy of conventional ultrasound, SWE and CEUS multi-parameter ultrasound indicators to identify HCA and FNH, with an intent to provide useful information for clinical treatment.

HCA is an estrogen-dependent tumor that has been reported in previous studies in young women or men taking steroids[27-29]. In this study, the proportion of female

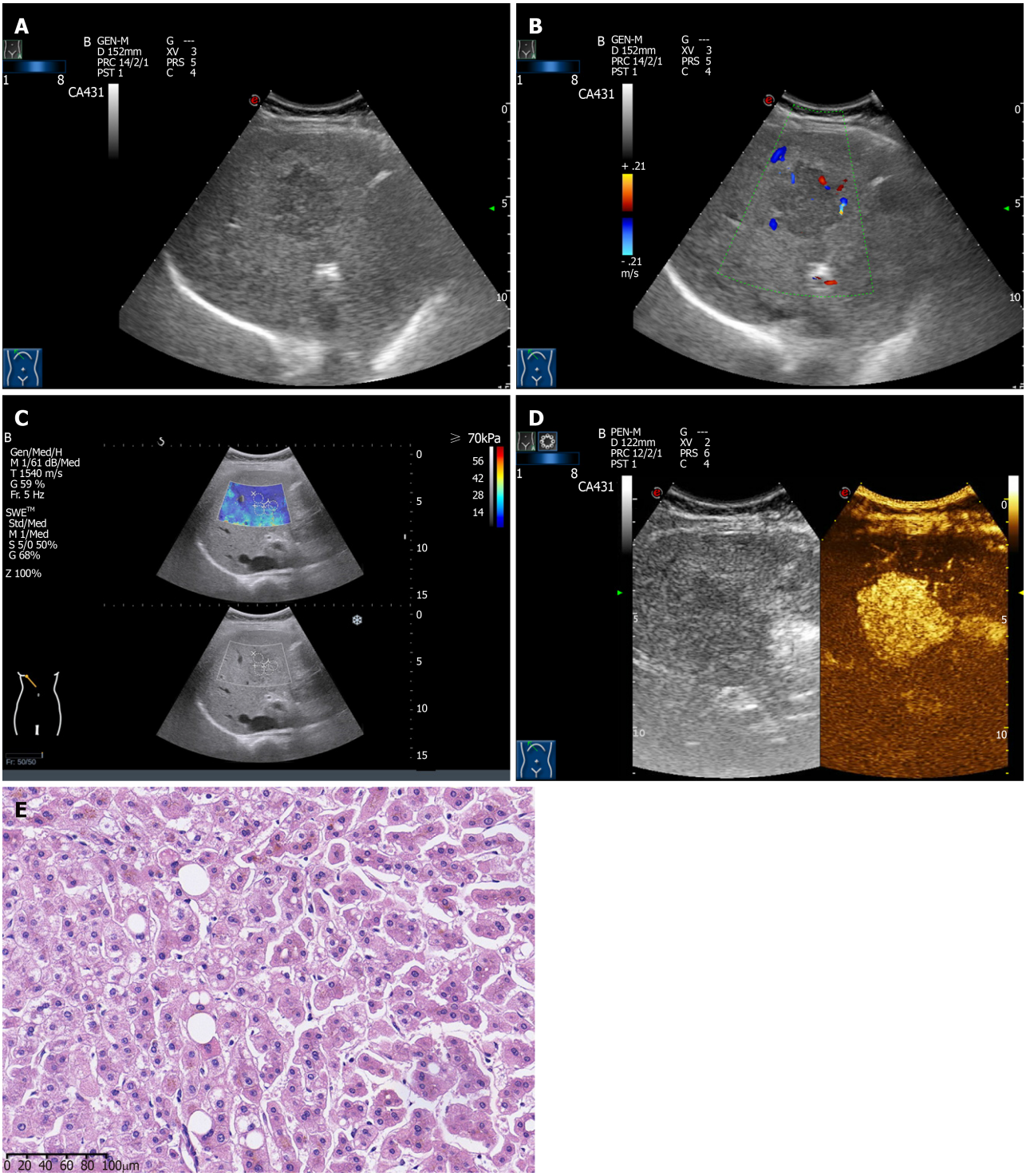

Figure 1 Ultrasonographic and pathological features of hepatocellular adenoma. A: Gray-scale ultrasound image of Hepatocellular adenoma (HCA); B: Color doppler flow Imaging image features of HCA; C: Shear wave elastography image features of HCA; D: Contrast-enhanced ultrasound image features of HCA; E: Pathological features of HCA.

patients with HCA was higher than that of FNH patients. However, there was no significant difference between the two groups in other clinical data, such as the history of viral infection, serological markers for evaluating liver function, and tumor markers (*e.g.*, AFP). It is difficult to identify HCA and FNH solely through clinical data and laboratory examinations[30]. According to pathological diagnostic criteria, we learned that the typical FNH lesions are nodular, with hyperplastic fibrous tissue, small blood vessels and bile duct structures. Stellate scars can be found in some FNH lesions. The tumor cells of HCA are similar to the surrounding normal liver cells. The center of the tumor may be accompanied by necrosis or hemorrhage. Some HCA lesions had scattered and lumen-expanded small blood vessels. However, there is no

Table 2 Comparison of ultrasound characteristics between hepatocellular adenoma group and focal nodular hyperplasia group

		HCA group, *n* = 31	FNH group, *n* = 50	t/χ^2 value	*P* value
Diameter in cm		3.37 ± 1.87	3.29 ± 1.58	0.206	0.837
Lesion location	Liver right lobe	24	36	0.293	0.589
	Liver left lobe	7	14		
Lesion echo	Low	9	31	11.637	0.009
	Equal	5	9		
	High	14	10		
	Mixed	2	0		
Lesion property	Solid	18	16	6.202	0.045
	Cystic	9	23		
	Mixed	3	11		
Lesion morphology	Regular	27	44	0.014	0.904
	Irregular	4	6		
Lesion boundary	Clear	27	47	1.155	0.282
	Unclear	4	3		
Lesion capsule	With capsule	30	46	0.753	0.386
	Without capsule	1	4		
Lesion internal echo	Uniform	26	43	0.069	0.793
	Non-uniform	5	7		
Microcalcification	No	30	48	0.032	0.858
	Yes	1	2		
Posterior echo	No echo attenuation	31	48	1.271	0.260
	Echo attenuation	0	2		
Lesion blood flow	No blood flow	7	20	4.870	0.088
	Spotted blood flow	18	27		
	Strip blood flow	6	3		
SWE	YM value in kPa	14.39 ± 7.28	29.27 ± 12.38	6.065	0.000
	YM ratio	3.73 ± 1.14	4.89 ± 1.99	2.770	0.007
TIC Quantitative analysis	PI-BI, dB	21.84 ± 8.83	20.18 ± 9.38	0.791	0.431
	ET, s	18.02 ± 5.88	20.27 ± 8.39	1.306	0.195
	TIC increasing slop	1.84 ± 0.62	1.72 ± 0.23	1.241	0.218
	TIC decreasing slop	0.31 ± 0.09	0.14 ± 0.07	9.510	0.000

HCA: Hepatocellular adenoma; FNH: Focal nodular hyperplasia; YM: Young's modulus; TIC: Time intense curve; ET: Enhancement time; PI-BI: Peak intensity background intensity; SWE: Shear wave elastography

portal area, portal vein, small bile duct branches, nuclear fission phase, or complete bile duct structures in HCA lesions. The presence of a complete portal system and bile duct structure is a major feature in identifying HCA and FNH. Histopathological examination is an invasive examination and cannot be used as a routine examination, although it can clearly distinguish HCA and FNH. Therefore, it is important to explore a non-invasive and simple imaging examination method to identify HCA and FNH.

This study compared the gray-scale ultrasound, SWE and CEUS indicators between the HCA group and the FNH group in order to explore the potential identification indicators of HCA and FNH. It revealed that the ratio of high echo HCA lesions was higher than that of FNH. We believe that this is due to the fact that HCA tumor cells are rich in glycogen and fat, and the high fat content makes a high echo. The study of Hasab *et al*[31] found that although HCA lesions were mostly in high echo types, their ultrasound performance also varies. Because the blood supply of HCA lesions is from the surrounding large blood vessels rather than the central artery, necrosis or hemorrhage is likely to occur in the tumor, and the site of necrosis or hemorrhage will appear as a no echo area. In addition, due to fibrous tissue hyperplasia, the stellate scars of FNH also represent as high echo, which is easily confused in the differential diagnosis of conventional ultrasound. The present study also found that lesion boundary, morphology, blood flow signals and other indicators of HCA and FNH were not significantly different. It indicated that the identification of HCA and FNH

Table 3 Multivariate logistic regression analysis of hepatocellular adenoma identification

	B	SE	Wald	*P* value	OR	95%CI	
						Lower limit	Upper limit
Gender	0.284	0.354	2.394	0.086	1.328	0.664	2.658
Lesion echo	0.977	0.157	7.967	0.000	2.657	1.953	3.614
Lesion property	0.427	0.964	1.234	0.137	1.532	0.232	10.135
YM value	- 0.289	0.108	6.567	0.000	0.749	0.606	0.926
YM ratio	- 0.154	0.135	1.436	0.134	0.857	0.658	1.117
TIC decreasing slope	1.673	0.284	5.829	0.000	5.328	3.054	9.296

YM: Young's modulus; TIC: Time intense curve.

solely by conventional gray-scale ultrasound was difficult.

The role of CEUS in the diagnosis of FNH has been recognized[32-34]. In the FNH group of the present study, the enhancement mode was mostly radioactively filled from the center to the periphery. The enhancement mode was slightly higher or of equal enhancement in the delayed phase, and some FNH had stellate scars. This is because the FNH blood supply is distributed centrally to the surrounding area, and the blood vessels are derived from the hepatic artery and the portal vein. During the portal vein phase, the contrast agent can be supplemented by the portal venous system, so it is called "fast-forward and slow-out"[35]. The enhancement mode of the HCA group was mostly peripheral-centered filling. Part of the HCA had a filling defect, that is, an ischemic necrotic area. The TIC decreasing slope of the HCA group was significantly higher than that of the FNH group. This is because the HCA tumor is surrounded by abundant peripheral blood vessels, and the branches of the blood vessels are infiltrated into the tumor for feeding. The contrast agent is filled with blood from the periphery to the center. If the lesion is large, the middle region is prone to lack blood supply and become necrotic, forming a filling defect. Because HCA lacks the portal system, its feeding vessels are derived from the hepatic artery. Hence the contrast agent is not supplemented during the portal vein phase. This enhanced mode is called "fast forward and fast out"[36]. In the FNH lesion, the portal vein was absent in the stellate scar, which was formed by fibrous tissue. Thus, the stellate filling defect area would appear in the CEUS. Nevertheless, HCA and FNH can be initially identified based on the difference in the two groups of CEUS findings. Guo *et al*[37] have found that the typical CEUS enhancement of FNH can also be found in HCA. Choi *et al*[38] also reported misdiagnosis in cases of HCA by CEUS[38]. Therefore, it is not accurate to identify HCA and FNH solely by utilizing CEUS.

SWE has been widely used in the differential diagnosis of benign and malignant liver lesions in recent years[39,40]. It was applied in the differential diagnosis of HCA and FNH in this study. The results found that the YM value and YM ratio in the HCA group were significantly lower than those in the FNH group, indicating that the lesion hardness in the HCA group was significantly lower than that in the FNH group. This is because most FNHs have stellate scars formed by coarse fibers. These scars divide the tissue into multiple small nodules. There is hyperplastic fibrous tissue, thickened blood vessel walls and hyperplastic bile ducts among the small nodules. Therefore, the fibrous tissue content in FNH is increased, and the tissue hardness is increased[41]. On the other hand, HCA is mainly composed of hepatocytes rich in glycogen and lipids. The fibrous tissue content is rare. Moreover, HCA lesion lack portal vein structure and bile ducts, often including ischemic necrosis. These all lead to a decrease in the hardness value of the HCA lesion[42-44].

According to the analysis results of the ROC curve in this study, gray-scale ultrasound, SWE and CEUS had their own advantages and disadvantages in identifying HCA and FNH. The lesion echo, YM value, and TIC decreasing slope could be used to identify HCA and FNH. Among them, YM value has the highest accuracy in identifying HCA. The AUC of HCA was 0.891, and the sensitivity was 92.16%. This suggested that the differential diagnosis of HCA and FNH by YM value is not prone to missed diagnosis. However, its specificity is low (73.28%), suggesting that the differential diagnosis of the YM value would result in a certain misdiagnosis rate. The AUC of the three indicators were all < 0.9, indicating that the accuracy of gray-scale ultrasound, SWE and CEUS for individually identifying HCA and FNH is limited. Therefore, this study combined the lesion echo, YM value, and TIC decreasing slope based on the logistic regression model. The combined diagnosis

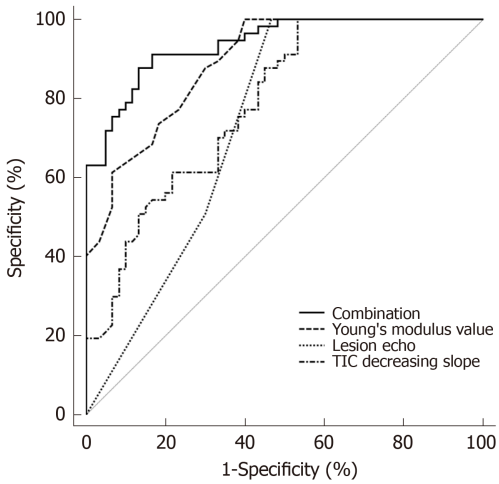

Figure 2 ROC curve analysis of Young's modulus value, time intense curve decreasing slope, lesion echo and their combination in the differential diagnosis of hepatocellular adenoma and focal nodular hyperplasia.

found that the AUC reached 0.938, which was higher than the AUC of these single indicators, indicating that the accuracy of the combined identification of the three indicators was the best. The combination of lesion echo, YM value and TIC decreasing slop in the differential diagnosis of HCA and FNH will hopefully be used in the clinic.

There are still shortcomings in this study. The SWE in this study was susceptible to the depth of the lesion and the operator. Hence, there is an inevitable error in the results. In addition, there is limited attention to this disease in the clinic because HCA is relatively rare and less malignant[45-50]. Thus, several patients in this study were not included because of incomplete clinical data, resulting in a limited sample size. Following this study, we expect to conduct further research on HCA in multiple centers, which will provide more useful information for clinical diagnosis through analyzing more specific data.

In conclusion, the combination of lesion echo, YM value and TIC decreasing slop in multi-parameter ultrasound indicators based on logistic regression has high clinical guiding value for the differential diagnosis of HCA and FNH.

Table 4 ROC curve analysis of multiple ultrasound parameters in the differential diagnosis of hepatocellular adenoma and focal nodular hyperplasia

	AUC	95%CI	Cut-off point	Sensitivity, %	Specificity, %
YM value	0.891[a]	0.820-0.941	23.26	92.16	73.28
TIC decreasing slope	0.785[a]	0.700-0.856	0.23	82.47	66.39
Lesion echo	0.676[a]	0.583-0.759	3	40.35	93.82
Combination	0.938	0.878-0.974	0.540	91.23	83.33

[a]$P < 0.05$. YM: Young's modulus; TIC: Time intense curve.

ARTICLE HIGHLIGHTS

Research background

Hepatocellular adenoma (HCA) is prone to secondary hemorrhage, and has a certain tendency towards malignant transformation. It needs to be closely observed and surgically removed if necessary. Focal nodular hyperplasia (FNH), which often needs to be differentiated, is a vascular malformation lesion, which is not a true tumor and has a tendency to spontaneously resolve, so conservative treatment can be adopted. The treatment methods and prognosis of them are quite different, but they are not easy to clinically identify. Therefore, it is of great significance to explore effective identification methods for them.

Research motivation

Current studies have shown that biochemical indicators do not have obvious advantages in identifying HCA and FNH. In imaging methods, it is difficult to distinguish the difference by using ultrasound. Recent studies have shown that contrast enhanced ultrasound (CEUS) can be used to diagnose HCA, but the diagnostic accuracy of FNH is low. It revealed that the value of differential diagnosis using conventional ultrasound, or CEUS individually, is limited. In recent years, shear wave elastography (SWE) has been widely used in the identification of benign and malignant tumors in the liver, but there are few applications for the differential diagnosis of HCA and FNH. Therefore, methods for identifying HAC and FNH are still lacking in the clinic.

Research objectives

In order to explore effective methods for identifying HCA and FNH, we will analyze the routine clinical indicators, including Doppler ultrasound, CEUS and SWE, in HCA and FNH patients. Logistic regression analysis will be used to analyze the significance of combined diagnosis of multi-parameter ultrasound indicators for improving the differential diagnosis of HCA and FNH.

Research methods

The study included 31 patients with HCA, and 50 patients with FNH. The clinical data of the two groups were recorded, and conventional ultrasound, CEUS, and SWE examinations were performed, and the ultrasound parameters such as lesion position, boundary echo, value and ratio of Young's modulus (YM), slope of TIC curve, *etc* were recorded. Multivariate regression analysis was used to screen potential indicators for the differential diagnosis of HCA and FNH. A ROC curve was used to evaluate the accuracy of potential indicators in differential diagnosis. A logistic regression model was used to establish a combination to explore the accuracy of differential diagnosis.

Research results

Multivariate regression analysis showed that lesion echo ($P = 0.000$), YM value ($P = 0.000$) and TIC decreasing slope ($P = 0.000$) were the potential indicators for identifying HCA and FNH. The accuracy of differential diagnosis of YM value is the highest, but its AUC is still less than 0.9. It is suggested that although the lesion echo, YM value and TIC decreasing slope were the influencing factors of HCA, the accuracy of differential diagnosis using conventional ultrasound, SWE and CEUS alone was limited. Further logistic regression results showed that the accuracy of the combined diagnosis of three indicators (AUC = 0.938) was significantly higher than the AUC of lesion echo (AUC = 0.676), YM value (AUC = 0.891), and TIC decreasing slope (AUC = 0.785). It is suggested that the accuracy of the combination of the three indicators is the best. The combined diagnosis of multi-parameter ultrasound can significantly improve the accuracy of differential diagnosis between HCA and FNH.

Research conclusions

Multi-parameter ultrasound in the differential diagnosis of HCA and FNH plays an important role. The combination of lesion echo, YM value and TIC decreasing slope can significantly improve the accuracy of differential diagnosis.

Research perspectives

In order to avoid the limitation of HCA patient cases, as well as the influence of the depth of the

lesion and operator in SWE defection. This study plans to further develop a multicenter study on HCA to improve diagnosis accuracy. The multi-center large sample study will further reveal the role of multi-parameter ultrasound in the differential diagnosis of HCA and FNH, and further improve the accuracy of the diagnosis.

REFERENCES

1 **Zhang G**, Wang M, Duan F, Yuan K, Li K, Yan J, Chang Z. Transarterial embolization with bleomycin for symptomatic hepatic focal nodular hyperplasia. *Diagn Interv Radiol* 2017; **23**: 66-70 [PMID: 27910813 DOI: 10.5152/dir.2016.16061]

2 **Roncalli M**, Sciarra A, Tommaso LD. Benign hepatocellular nodules of healthy liver: focal nodular hyperplasia and hepatocellular adenoma. *Clin Mol Hepatol* 2016; **22**: 199-211 [PMID: 27189732 DOI: 10.3350/cmh.2016.0101]

3 **Dioguardi Burgio M**, Ronot M, Salvaggio G, Vilgrain V, Brancatelli G. Imaging of Hepatic Focal Nodular Hyperplasia: Pictorial Review and Diagnostic Strategy. *Semin Ultrasound CT MR* 2016; **37**: 511-524 [PMID: 27986170 DOI: 10.1053/j.sult.2016.08.001]

4 **Nault JC**, Couchy G, Balabaud C, Morcrette G, Caruso S, Blanc JF, Bacq Y, Calderaro J, Paradis V, Ramos J, Scoazec JY, Gnemmi V, Sturm N, Guettier C, Fabre M, Savier E, Chiche L, Labrune P, Selves J, Wendum D, Pilati C, Laurent A, De Muret A, Le Bail B, Rebouissou S, Imbeaud S; GENTHEP Investigators, Bioulac-Sage P, Letouzé E, Zucman-Rossi J. Molecular Classification of Hepatocellular Adenoma Associates With Risk Factors, Bleeding, and Malignant Transformation. *Gastroenterology* 2017; **152**: 880-894.e6 [PMID: 27939373 DOI: 10.1053/j.gastro.2016.11.042]

5 **Nguyen TB**, Roncalli M, Di Tommaso L, Kakar S. Combined use of heat-shock protein 70 and glutamine synthetase is useful in the distinction of typical hepatocellular adenoma from atypical hepatocellular neoplasms and well-differentiated hepatocellular carcinoma. *Mod Pathol* 2016; **29**: 283-292 [PMID: 26769138 DOI: 10.1038/modpathol.2015.162]

6 **Dong Y**, Zhu Z, Wang WP, Mao F, Ji ZB. Ultrasound features of hepatocellular adenoma and the additional value of contrast-enhanced ultrasound. *Hepatobiliary Pancreat Dis Int* 2016; **15**: 48-54 [PMID: 26818543 DOI: 10.1016/s1499-3872(15)60039-x]

7 **Henriet E**, Abou Hammoud A, Dupuy JW, Dartigues B, Ezzoukry Z, Dugot-Senant N, Leste-Lasserre T, Pallares-Lupon N, Nikolski M, Le Bail B, Blanc JF, Balabaud C, Bioulac-Sage P, Raymond AA, Saltel F. Argininosuccinate synthase 1 (ASS1): A marker of unclassified hepatocellular adenoma and high bleeding risk. *Hepatology* 2017; **66**: 2016-2028 [PMID: 28646562 DOI: 10.1002/hep.29336]

8 **Beppu T**, Nakagawa S, Nitta H, Okabe H, Kaida T, Imai K, Hayashi H, Koga Y, Kuramoto K, Hashimoto D, Yamashita YI, Chikamoto A, Ishiko T, Baba H. The Number of Positive Tumor Marker Status Is Beneficial for the Selection of Therapeutic Modalities in Patients with Hepatocellular Carcinoma. *J Clin Transl Hepatol* 2017; **5**: 165-168 [PMID: 28660154 DOI: 10.14218/JCTH.2016.00055]

9 **Liu D**, Liu P, Cao L, Zhang Q, Chen Y. Screening the key genes of hepatocellular adenoma via microarray analysis of DNA expression and methylation profiles. *Oncol Lett* 2017; **14**: 3975-3980 [PMID: 28943905 DOI: 10.3892/ol.2017.6673]

10 **Rübenthaler J**, Paprottka KJ, Hameister E, Hoffmann K, Joiko N, Reiser M, Rjosk-Dendorfer D, Clevert DA. Diagnostic accuracy of contrast-enhanced ultrasound (CEUS) in monitoring vascular complications in patients after liver transplantation - diagnostic performance compared with histopathological results. *Clin Hemorheol Microcirc* 2017; **66**: 311-316 [PMID: 28527202 DOI: 10.3233/CH-179105]

11 **Kono Y**, Lyshchik A, Cosgrove D, Dietrich CF, Jang HJ, Kim TK, Piscaglia F, Willmann JK, Wilson SR, Santillan C, Kambadakone A, Mitchell D, Vezeridis A, Sirlin CB. Contrast Enhanced Ultrasound (CEUS) Liver Imaging Reporting and Data System (LI-RADS®): the official version by the American College of Radiology (ACR). *Ultraschall Med* 2017; **38**: 85-86 [PMID: 28249328 DOI: 10.1055/s-0042-124369]

12 **Huf S**, Platz Batista da Silva N, Wiesinger I, Hornung M, Scherer MN, Lang S, Stroszczynski C, Fischer T, Jung EM. Analysis of Liver Tumors Using Preoperative and Intraoperative Contrast-Enhanced Ultrasound (CEUS/IOCEUS) by Radiologists in Comparison to Magnetic Resonance Imaging and Histopathology. *Rofo* 2017; **189**: 431-440 [PMID: 28449169 DOI: 10.1055/s-0042-124347]

13 **Ferraioli G**, Meloni MF. Contrast-enhanced ultrasonography of the liver using SonoVue. *Ultrasonography* 2018; **37**: 25-35 [PMID: 28830058 DOI: 10.14366/usg.17037]

14 **Taimr P**, Bröker MEE, Dwarkasing RS, Hansen BE, de Knegt RJ, De Man RA, IJzermans JNM. A Model-Based Prediction of the Probability of Hepatocellular Adenoma and Focal Nodular Hyperplasia Based on Characteristics on Contrast-Enhanced Ultrasound. *Ultrasound Med Biol* 2017; **43**: 2144-2150 [PMID: 28743375 DOI: 10.1016/j.ultrasmedbio.2017.05.011]

15 **Piscaglia F**, Salvatore V, Mulazzani L, Cantisani V, Schiavone C. Ultrasound Shear Wave Elastography for Liver Disease. A Critical Appraisal of the Many Actors on the Stage. *Ultraschall Med* 2016; **37**: 1-5 [PMID: 26871407 DOI: 10.1055/s-0035-1567037]

16 **Bende F**, Sporea I, Sirli R, Popescu A, Mare R, Miutescu B, Lupusoru R, Moga T, Pienar C. Performance of 2D-SWE.GE for predicting different stages of liver fibrosis, using Transient Elastography as the reference method. *Med Ultrason* 2017; **19**: 143-149 [PMID: 28440347 DOI: 10.11152/mu-910]

17 **Dong Y**, Sirli R, Ferraioli G, Sporea I, Chiorean L, Cui X, Fan M, Wang WP, Gilja OH, Sidhu PS, Dietrich CF. Shear wave elastography of the liver - review on normal values. *Z Gastroenterol* 2017; **55**: 153-166 [PMID: 28192849 DOI: 10.1055/s-0042-117226]

18 **Gerber L**, Fitting D, Srikantharajah K, Weiler N, Kyriakidou G, Bojunga J, Schulze F, Bon D, Zeuzem S, Friedrich-Rust M. Evaluation of 2D- Shear Wave Elastography for Characterisation of Focal Liver Lesions. *J Gastrointestin Liver Dis* 2017; **26**: 283-290 [PMID: 28922441 DOI: 10.15403/jgld.2014.1121.263.dsh]

19 **Xie DY**, Ren ZG, Zhou J, Fan J, Gao Q. Critical appraisal of Chinese 2017 guideline on the management of hepatocellular carcinoma. *Hepatobiliary Surg Nutr* 2017; **6**: 387-396 [PMID: 29312973 DOI: 10.21037/hbsn.2017.11.01]

20 **Tian WS**, Lin MX, Zhou LY, Pan FS, Huang GL, Wang W, Lu MD, Xie XY. Maximum Value Measured by 2-D Shear Wave Elastography Helps in Differentiating Malignancy from Benign Focal Liver Lesions. *Ultrasound Med Biol* 2016; **42**: 2156-2166 [PMID: 27283039 DOI: 10.1016/j.ultrasmedbio.2016.05.002]

21 **Klompenhouwer AJ**, IJzermans JNM. Malignant potential of hepatocellular adenoma. *Liver Int* 2017; **37**: 966-967 [PMID: 28635168 DOI: 10.1111/liv.13449]

22 **Klompenhouwer AJ**, de Man RA, Thomeer MG, Ijzermans JN. Management and outcome of hepatocellular adenoma with massive bleeding at presentation. *World J Gastroenterol* 2017; **23**: 4579-4586 [PMID: 28740346 DOI: 10.3748/wjg.v23.i25.4579]

23 **Zhang HT**, Gao XY, Xu QS, Chen YT, Song YP, Yao ZW. Evaluation of the characteristics of hepatic focal nodular hyperplasia: correlation between dynamic contrast-enhanced multislice computed tomography and pathological findings. *Onco Targets Ther* 2016; **9**: 5217-5224 [PMID: 27578988 DOI: 10.2147/OTT.S103647]

24 **Grieser C**, Steffen IG, Kramme IB, Bläker H, Kilic E, Perez Fernandez CM, Seehofer D, Schott E, Hamm B, Denecke T. Gadoxetic acid enhanced MRI for differentiation of FNH and HCA: a single centre experience. *Eur Radiol* 2014; **24**: 1339-1348 [PMID: 24658870 DOI: 10.1007/s00330-014-3144-7]

25 **Albrecht T**, Blomley M, Bolondi L, Claudon M, Correas JM, Cosgrove D, Greiner L, Jäger K, Jong ND, Leen E, Lencioni R, Lindsell D, Martegani A, Solbiati L, Thorelius L, Tranquart F, Weskott HP, Whittingham T; EFSUMB Study Group. Guidelines for the use of contrast agents in ultrasound. January 2004. *Ultraschall Med* 2004; **25**: 249-256 [PMID: 15300497 DOI: 10.1055/s-2004-813245]

26 **Thiele M**, Madsen BS, Procopet B, Hansen JF, Møller LMS, Detlefsen S, Berzigotti A, Krag A. Reliability Criteria for Liver Stiffness Measurements with Real-Time 2D Shear Wave Elastography in Different Clinical Scenarios of Chronic Liver Disease. *Ultraschall Med* 2017; **38**: 648-654 [PMID: 27273177 DOI: 10.1055/s-0042-108431]

27 **Sinclair M**, Schelleman A, Sandhu D, Angus PW. Regression of hepatocellular adenomas and systemic inflammatory syndrome after cessation of estrogen therapy. *Hepatology* 2017; **66**: 989-991 [PMID: 28295483 DOI: 10.1002/hep.29151]

28 **Taniai-Riya E**, Miyajima K, Kakimoto K, Ohta T, Yasui Y, Kemmochi Y, Anagawa-Nakamura A, Toyoda K, Takahashi A, Shoda T. Hepatocellular adenoma with severe fatty change in a male Spontaneously Diabetic Torii rat. *J Toxicol Pathol* 2017; **30**: 69-73 [PMID: 28190927 DOI: 10.1293/tox.2016-0051]

29 **Khaoudy I**, Rebibo L, Regimbeau JM. Is bariatric surgery a potential new treatment for large inflammatory hepatocellular adenomas in obese patients? *Surg Obes Relat Dis* 2018; **14**: 535-538 [PMID: 29555032 DOI: 10.1016/j.soard.2018.01.006]

30 **Reizine E**, Amaddeo G, Pigneur F, Baranes L, Legou F, Mulé S, Zegai B, Roche V, Laurent A, Rahmouni A, Calderaro J, Luciani A. Quantitative correlation between uptake of Gd-BOPTA on hepatobiliary phase and tumor molecular features in patients with benign hepatocellular lesions. *Eur Radiol* 2018; **28**: 4243-4253 [PMID: 29721686 DOI: 10.1007/s00330-018-5438-7]

31 **Hasab Allah M**, Salama RM, Marie MS, Mandur AA, Omar H. Utility of point shear wave elastography in characterisation of focal liver lesions. *Expert Rev Gastroenterol Hepatol* 2018; **12**: 201-207 [PMID: 29219625 DOI: 10.1080/17474124.2018.1415144]

32 **Naganuma H**, Ishida H, Ogawa M, Watanabe Y, Watanabe D, Ohyama Y, Watanabe T. Focal nodular hyperplasia: our experience of 53 Japanese cases. *J Med Ultrason (2001)* 2017; **44**: 79-88 [PMID: 27550510 DOI: 10.1007/s10396-016-0734-9]

33 **Rousseau C**, Ronot M, Vilgrain V, Zins M. Optimal visualization of focal nodular hyperplasia: quantitative and qualitative evaluation of single and multiphasic arterial phase acquisition at 1.5 T MR imaging. *Abdom Radiol (NY)* 2016; **41**: 990-1000 [PMID: 27193796 DOI: 10.1007/s00261-015-0630-6]

34 **Sheng R**, Palm V, Mayer P, Mokry T, Berger AK, Weiss KH, Longerich T, Kauczor HU, Weber TF. Gadoxetic Acid-Enhanced Hepatobiliary-Phase Magnetic Resonance Imaging for Delineation of Focal Nodular Hyperplasia: Superiority of High-Flip-Angle Imaging. *J Comput Assist Tomogr* 2018; **42**: 667-674 [PMID: 30119067 DOI: 10.1097/RCT.0000000000000777]

35 **Sun XL**, Yao H, Men Q, Hou KZ, Chen Z, Xu CQ, Liang LW. Combination of acoustic radiation force impulse imaging, serological indexes and contrast-enhanced ultrasound for diagnosis of liver lesions. *World J Gastroenterol* 2017; **23**: 5602-5609 [PMID: 28852319 DOI: 10.3748/wjg.v23.i30.5602]

36 **Kong WT**, Wang WP, Huang BJ, Ding H, Mao F, Si Q. Contrast-enhanced ultrasound in combination with color Doppler ultrasound can improve the diagnostic performance of focal nodular hyperplasia and hepatocellular adenoma. *Ultrasound Med Biol* 2015; **41**: 944-951 [PMID: 25701530 DOI: 10.1016/j.ultrasmedbio.2014.11.012]

37 **Guo Y**, Li W, Cai W, Zhang Y, Fang Y, Hong G. Diagnostic Value of Gadoxetic Acid-Enhanced MR Imaging to Distinguish HCA and Its Subtype from FNH: A Systematic Review. *Int J Med Sci* 2017; **14**: 668-674 [PMID: 28824299 DOI: 10.7150/ijms.17865]

38 **Choi IY**, Lee SS, Sung YS, Cheong H, Lee H, Byun JH, Kim SY, Lee SJ, Shin YM, Lee MG. Intravoxel incoherent motion diffusion-weighted imaging for characterizing focal hepatic lesions: Correlation with lesion enhancement. *J Magn Reson Imaging* 2017; **45**: 1589-1598 [PMID: 27664970 DOI: 10.1002/jmri.25492]

39 **Grgurevic I**, Bokun T, Salkic NN, Brkljacic B, Vukelić-Markovic M, Stoos-Veic T, Aralica G, Rakic M, Filipec-Kanizaj T, Berzigotti A. Liver elastography malignancy prediction score for noninvasive characterization of focal liver lesions. *Liver Int* 2018; **38**: 1055-1063 [PMID: 29028279 DOI: 10.1111/liv.13611]

40 **Jiao Y**, Dong F, Wang H, Zhang L, Xu J, Zheng J, Fan H, Gan H, Chen L, Li M. Shear wave elastography imaging for detecting malignant lesions of the liver: a systematic review and pooled meta-analysis. *Med Ultrason* 2017; **19**: 16-22 [PMID: 28180192 DOI: 10.11152/mu-925]

41 **Akdoğan E**, Yılmaz FG. The role of acoustic radiation force impulse elastography in the differentiation of benign and malignant focal liver masses. *Turk J Gastroenterol* 2018; **29**: 456-463 [PMID: 30249561 DOI: 10.5152/tjg.2018.11710]

42 **Mulazzani L**, Salvatore V, Ravaioli F, Allegretti G, Matassoni F, Granata R, Ferrarini A, Stefanescu H, Piscaglia F. Point shear wave ultrasound elastography with Esaote compared to real-time 2D shear wave elastography with supersonic imagine for the quantification of liver stiffness. *J Ultrasound* 2017; **20**: 213-225 [PMID: 28900522 DOI: 10.1007/s40477-017-0260-7]

43 **Dietrich CF**, Dong Y. Shear wave elastography with a new reliability indicator. *J Ultrason* 2016; **16**: 281-287 [PMID: 27679731 DOI: 10.15557/JoU.2016.0028]

44 **Ronot M**, Di Renzo S, Gregoli B, Duran R, Castera L, Van Beers BE, Vilgrain V. Characterization of fortuitously discovered focal liver lesions: additional information provided by shearwave elastography. *Eur Radiol* 2015; **25**: 346-358 [PMID: 25231131 DOI: 10.1007/s00330-014-3370-z]

45 **Kim JW**, Lee CH, Kim SB, Park BN, Park YS, Lee J, Park CM. Washout appearance in Gd-EOB-DTPA-enhanced MR imaging: A differentiating feature between hepatocellular carcinoma with paradoxical uptake on the hepatobiliary phase and focal nodular hyperplasia-like nodules. *J Magn Reson Imaging*

2017; **45**: 1599-1608 [PMID: 27726242 DOI: 10.1002/jmri.25493]
46 **Taibbi A**, Brancatelli G, Matranga D, Midiri M, Lagalla R, Bartolotta TV. Focal nodular hyperplasia: a weight-based, intraindividual comparison of gadobenate dimeglumine and gadoxetate disodium-enhanced MRI. *Diagn Interv Radiol* 2019; **25**: 95-101 [PMID: 30860073 DOI: 10.5152/dir.2019.18165]
47 **Dietrich CF**, Bamber J, Berzigotti A, Bota S, Cantisani V, Castera L, Cosgrove D, Ferraioli G, Friedrich-Rust M, Gilja OH, Goertz RS, Karlas T, de Knegt R, de Ledinghen V, Piscaglia F, Procopet B, Saftoiu A, Sidhu PS, Sporea I, Thiele M. EFSUMB Guidelines and Recommendations on the Clinical Use of Liver Ultrasound Elastography, Update 2017 (Short Version). *Ultraschall Med* 2017; **38**: 377-394 [PMID: 28407654 DOI: 10.1055/s-0043-103955]
48 **Herrmann E**, de Lédinghen V, Cassinotto C, Chu WC, Leung VY, Ferraioli G, Filice C, Castera L, Vilgrain V, Ronot M, Dumortier J, Guibal A, Pol S, Trebicka J, Jansen C, Strassburg C, Zheng R, Zheng J, Francque S, Vanwolleghem T, Vonghia L, Manesis EK, Zoumpoulis P, Sporea I, Thiele M, Krag A, Cohen-Bacrie C, Criton A, Gay J, Deffieux T, Friedrich-Rust M. Assessment of biopsy-proven liver fibrosis by two-dimensional shear wave elastography: An individual patient data-based meta-analysis. *Hepatology* 2018; **67**: 260-272 [PMID: 28370257 DOI: 10.1002/hep.29179]
49 **Xie LT**, Yan CH, Zhao QY, He MN, Jiang TA. Quantitative and noninvasive assessment of chronic liver diseases using two-dimensional shear wave elastography. *World J Gastroenterol* 2018; **24**: 957-970 [PMID: 29531460 DOI: 10.3748/wjg.v24.i9.957]
50 **Nault JC**, Paradis V, Cherqui D, Vilgrain V, Zucman-Rossi J. Molecular classification of hepatocellular adenoma in clinical practice. *J Hepatol* 2017; **67**: 1074-1083 [PMID: 28733222 DOI: 10.1016/j.jhep.2017.07.009]

Published By Baishideng Publishing Group Inc
7041 Koll Center Parkway, Suite 160, Pleasanton, CA 94566, USA
Telephone: +1-925-2238242
E-mail: bpgoffice@wjgnet.com
Help Desk:https://www.f6publishing.com/helpdesk
https://www.wjgnet.com